

Article

Inorganic Flame-Retardant Coatings Based on Magnesium Potassium Phosphate Hydrate

Sin-Nan Chen, Ching Lin, Hao-Lun Hsu, Xin-Han Chen, Yu-Chang Huang, Tar-Hwa Hsieh *, Ko-Shan Ho * and Yu-Jun Lin

Department of Chemical and Materials Engineering, National Kaohsiung University of Science and Technology, Kaohsiung 807618, Taiwan; h722655@gmail.com (S.-N.C.); f110146145@nkust.edu.tw (C.L.); c108146220@nkust.edu.tw (H.-L.H.); c106146220@nkust.edu.tw (X.-H.C.); ych@nkust.edu.tw (Y.-C.H.); c108146243@nkust.edu.tw (Y.-J.L.)

* Correspondence: thh@nkust.edu.tw (T.-H.H.); hks@nkust.edu.tw (K.-S.H.)

Abstract: A magnesium potassium phosphate hydrate-based flame-retardant coating (MKPC) is formulated by dead-burnt magnesium oxide (magnesia) and potassium dihydrogen phosphate (KH_2PO_4), behaving as a matrix. Constituents of the MKPC include wollastonite, vermiculite, aluminum fluoride, aluminum trihydroxide, and calcium carbonate. Some of the ingredients inter-react to produce mullite whiskers at high temperatures, despite an acid-base hydration induced reaction between magnesia and KH_2PO_4 . The MKPC's thermal, corrosion-resistant, mechanical, and flame-resistant properties were analyzed using scanning electron microscopy, electrochemical corrosion testing, compression testing, thermogravimetric analysis, and freeze/thaw tests. The results show that with the molar ratio = 4 of magnesia to KH_2PO_4 , MKPC demonstrates lower thermal conductivity (0.19 W/m K), along with better corrosion resistance, stronger compressive strength (10.5 MPa), and higher bonding strength (6.62 kgf/cm²) to the steel substrate. Furthermore, acceptable additives to the formulation could enhance its flame-retardancy and increase its mechanical strength as well. Mullite whisker formed from the interaction of wollastonite, aluminum trihydroxide, and aluminum fluoride acts as an outer ceramic shield that enhances mechanical strength and compactness. In addition, Mg-containing minerals with calcium carbonate treated at high temperatures, transform into magnesium calcium carbonate after releasing CO_2 . At the optimum composition of MKPC (magnesia/ KH_2PO_4 molar ratio = 4; wollastonite:vermiculite = 20:10 wt.%; aluminum trihydroxide = 10 wt.%; and calcium carbonate = 5 wt.%), coated on a steel substrate, the flame-resistance limit results exhibit below 200 °C on the back surface of the steel substrate after one hour of flaming (ca. 1000 °C) on the other surface, and the flame-resistance rating results demonstrate only 420 °C on the back surface of the steel substrate after three hours of flaming (>1000 °C) on the other surface. Both requirements for the flame-resistance limit and three-hour flame-resistance rating are met with the optimum compositions, indicating that MKPC plays an effective role in establishing flame-retardancy.

Keywords: magnesium potassium phosphate hydrate-based flame-retardant coating; mullite whisker; flame-resistance limit; flame-resistance rating; ceramic shield; flame-retardancy



Citation: Chen, S.-N.; Lin, C.; Hsu, H.-L.; Chen, X.-H.; Huang, Y.-C.; Hsieh, T.-H.; Ho, K.-S.; Lin, Y.-J. Inorganic Flame-Retardant Coatings Based on Magnesium Potassium Phosphate Hydrate. *Materials* **2022**, *15*, 5317. <https://doi.org/10.3390/ma15155317>

Academic Editors: Fernando Gomes de Souza Junior and Diganta B. Das

Received: 4 July 2022

Accepted: 30 July 2022

Published: 2 August 2022

Publisher's Note: MDPI stays neutral with regard to jurisdictional claims in published maps and institutional affiliations.



Copyright: © 2022 by the authors. Licensee MDPI, Basel, Switzerland. This article is an open access article distributed under the terms and conditions of the Creative Commons Attribution (CC BY) license (<https://creativecommons.org/licenses/by/4.0/>).

1. Introduction

The topic of catastrophic fire has been around for decades, constantly causing massive loss of lives and resources. Therefore, passive flame-retardant coatings developed for steel-made construction materials play an important role in building construction. Generally, flame-retardant coatings are divided into organic [1] and inorganic [2] materials. The inorganic counterparts include intumescent [3] and non-intumescent coatings. In 2021, Chen et al. [4] reported a silicate-based intumescent flame-retardant coating, which showed remarkable results during firing. Even so, the practical requirements for water and weather resistance remain unmet. Therefore, silicate-based intumescent fire-retardant coatings are

considered more suitable for interior decoration applications as they can meet most of the requirements.

Another possible alternative to inorganic matrices are hydraulic binding materials such as magnesium potassium phosphate cements, which are known for their high adhesion properties [5,6], good corrosion resistance to steel substrates [7,8], and freeze-thaw resistance. Furthermore, it has been reported that the rapid acid-base hydration reaction of MgO with KH_2PO_4 in aqueous solution is dominated by the water-cement ratio [9] and the MgO/ KH_2PO_4 ratio [10,11], respectively.

Magnesium potassium phosphate cement has many excellent characteristics, such as rapid setting, high early strength, high fluidity, good volume stability, strong bonding strength to concrete substrates, and superior durability. Therefore, it has been applied in various fields such as the rehabilitation and repair of civil structures, the treatment of wastewater, and the stabilization of hazardous waste [12]. However, current studies on magnesium potassium phosphate cement mainly focus on the reaction and retardation mechanisms, the influencing factors on the properties of the magnesium potassium phosphate cement, and similar subjects. Some studies have shown that magnesium potassium phosphate cement has a high temperature resistance, but there are few reports on the use of magnesium potassium phosphate cement as a fire-retardant coating. Because most current fire-retardant coatings contain volatile organic components, they are expensive, toxic, and have low resistance to fire [5].

In the past, it has been reported in a small number of studies that magnesium potassium phosphate with flame-retardant properties can be used as a substrate for newly developed flame-retardant coatings [13,14]. However, these coatings also suffer from some disadvantages, such as poor mechanical strength and less flame-retardancy improvement in flame resistance, which demonstrates these coatings cannot easily be adapted to building material applications. Recently, Ding [5] suggested the incorporation of glass fiber or glass fiber powder as a mineral admixture into magnesium potassium phosphate cement for plywood fire-proof coating, which exhibited good spread fluidity, initial setting time, bonding strength, and fire-retardancy. CN 104230305 B [15] reported that a fire-proof coating based on magnesium potassium phosphate cement contains thermal insulation, inorganic material, and auxiliary agents, which suggests this coating can effectively replace traditional silicate cement and high-alumina cement for the inside wall of tunnels, to establish fire-retardancy. CN 104230305 B [16] described a fire-resistant coating based on magnesium potassium phosphate cement containing corundum sand, expanded perlite, and polypropylene fiber for steel structure coating. They pointed out this coating has a controllable setting time, hardens fast, cures at normal temperatures, is easy to preserve, is low-cost, has a higher bonding strength to the steel construction matrix, high mechanical strength, excellent fire-protecting performance, and good stability and endurance. Consequently, several mineral additives that can improve performance characteristics were selected in the formulations, including flame-resistance, toughness, mechanical strength, thermal shock resistance, weathering durability, etc. [17–19]. However, the thickness of magnesium potassium phosphate cement-based coatings layered in the substrate is still thicker (i.e., 15–20 mm), which may induce poor workability (slower construction and curing rate) and crack formation during the flame exposure. Despite these coatings meeting the requirements of the flame limit, which means that the magnesium potassium phosphate cement does not burn and that there is a time delay until the coated object begins to burn, it is very difficult to simulate the fire-retardancy of coatings under real flame conditions due to the lack of direct flame-resistance rating testing.

In consideration of these issues, our aim is to adopt ingredients that can be very effective in increasing the flame-retardancy of coatings for steel construction when exposed to flame. Additionally, proper thermal insulation additives (wollastonite and vermiculite) and functional additives (aluminum hydroxide, aluminum fluoride and calcium carbonate) selections are being implemented to enhance the anti-corrosion properties and overall mechanical strength. Therefore, as far as we understand, steel coated with the magne-

sium potassium phosphate hydrate-based flame-retardant coating (MKPC) can meet the requirements of steel construction for building material applications. In the present study, the MKPC's fire-retardancy, corrosion behavior, and mechanical strength were analyzed by means of a flame-resistance limit and a flame-resistance rating test method, the Tafel method and the universal machine test method, respectively. For easy and fast construction and curing, a thinner MKPC coating was also adopted.

2. Materials and Methods

2.1. Preparation of Magnesium Potassium Phosphate Hydrate

Magnesium oxide (MgO 90%, SiO₂ 5%, CaO 2.2%) and KH₂PO₄ (Taiwan Guosheng Plumbing Service Co., Ltd., Mailiao Township, Taiwan) were mixed in a molar ratio of 2–5 by a mechanical mixer. Water was then introduced during stirring at a weight ratio of 0.3 to the powder mixture. The resultant pastes prepared with various magnesia/KH₂PO₄ molar ratios were poured into molds and then cured at ambient temperatures.

2.2. Preparation of the MKPCs

The slurry described above contained mixtures of wollastonite (SiO₂ 50.77%, CaO 45.26%, MgO 1.29%) and vermiculite ((MgFe,Al)₃(Al,Si)₄O₁₀(OH)₂·4H₂O 30% weight percentage) with ratios of 20:10, 10:20 and 10:10, respectively, acting as insulation additives. Functional additives included 4 wt.% aluminum fluoride (of AlF₃·31/2H₂O, Emperor Chemical Co. Ltd., Taipei, Taiwan), 3–5 wt.% aluminum hydroxide (purity > 99%, particle size = 52 μm), and 3–10 wt.% calcium carbonate (ultra-pure reagent, precipitated). The MKPC pastes were prepared with a W/C ratio of 0.8 (W/C = 0.8), in which cement was based on the powder mixture. The MKPC was then brushed onto a steel substrate, creating a layer with a thickness of approximately 5 mm, and cured in the atmosphere.

2.3. Corrosion Characterization and Flame-Resistance Testing of the MKPCs

The chemical composition of the coating and the steel substrate, as well as the acronyms of the studied samples, are summarized in Tables 1 and 2. SEM was used to characterize the surface morphology of the MKPC. A potentiostat was used to detect the electrochemical corrosion. The MKPC was first coated to one side of a 3 cm × 3 cm cleaned SN400YB steel substrate to a thickness of 5 mm, applied by brushing; the other side was then sealed with paraffin and fixed to a 1 cm × 1 cm soaking area. The MKPC specimens were immersed in a 3.5 wt.% NaCl (aq) soaking solution after 24 h of curing. The polarization curve of the MKPC specimens was analyzed using an Autolab potentiostat, with Ag/AgCl and platinum as the reference and counter electrode; the scan rate was 0.5 mVs⁻¹ over a potential range of between −300 and +1200 mV. The density of the instantaneous corrosion current density (J_{cor} , expressed in mA cm⁻²) was calculated with Equation (1), and the corrosion rate, expressed as penetration rate (v_p , expressed in mm/year), was calculated with Equation (2) [20,21].

$$J_{\text{cor}} = (b_a \times b_c) / (2.303 (b_a + b_c) \times R_p) \quad (1)$$

$$v_p = 3.27 \times (A/Z) \times (J_{\text{cor}}/\rho) \quad (2)$$

where b_a and b_c represent the slope of the linear portion of the anodic branch and the cathodic branch, respectively. In the diagram $E = f(\log J)$; $R_p = (dE/dJ)$, E_{cor} is the polarization resistance (expressed in Ω cm²), A/z represents the electrochemical equivalent of the corroding metal (in this case, iron was considered because it is the component with the largest amount in the alloy, $A(\text{Fe}) = 55.85 \text{ g mol}^{-1}$, and $z = 2$), and ρ is density (for Fe, $\rho = 7.5 \text{ g cm}^{-3}$). The crystal structure and phase change at high temperatures of the MKPC at different calcination levels were analyzed by a Bruker D8 Advance X-ray diffractometer (Karlsruhe, Germany). A thermogravimetric analyzer (Simultaneous DTA-TGA, SDT 2960, TA Instruments, New Castle, DE, USA), was used to evaluate the thermal stability of the MKPC. The thermal conductivity of the MKPC was obtained using a TechMax Technical

Group Hot Disk Analyzer (TechMax Technical Co. Ltd., New Taipei, Taiwan). According to the Chinese specification (GB14907), the flammability limit of the MKPC (time required at ~250 °C) was found by using an alcohol blast burner at a temperature of ~1000 °C at a distance of ~6 cm from the MKPC. The thickness of the coating layered in the steel substrate was 5 mm, applied by brushing.

Table 1. The composition of the MKPC samples at M/P = 4 and W/C = 0.8.

Sample	Wollastonite (wt.%)	Vermiculite (wt.%)	Aerogel (wt.%)	Aluminum Fluoride (wt.%)	Aluminum Hydroxide (wt.%)	Metakaolin (wt.%)	Calcium Carbonate (wt.%)
A1	20	10	-	-	-	-	-
A2	10	20	-	-	-	-	-
A3	15	15	-	-	-	-	-
B1	20	10	3	-	-	-	-
B2	20	10	5	-	-	-	-
B3	20	10	10	-	-	-	-
C1	20	10	-	4	3	-	-
C2	20	10	-	4	5	-	-
C3	20	10	-	4	10	-	-
C4	20	10	-	4	15	-	-
D1	20	10	-	4	10	3	-
D2	20	10	-	4	10	5	-
D3	20	10	-	4	10	10	-
E1	20	10	-	4	10	-	3
E2	20	10	-	4	10	-	5
E3	20	10	-	4	10	-	10

Table 2. The composition of SN400YB, used as the steel substrate.

Composition	C	Si	Mn	P	S	B	Fe
Measured (wt.%)	0.2	0.35	0.6	0.03	0.015	0.0008	Balance

To find out the flame-retardancy rating, the prepared MKPC was adhered to a steel substrate and burned by a pilot flame (~1100 °C) at a distance of approximately 10 cm. A compressor machine with a dimension of 5 cm × 5 cm × 5 cm then tested the mechanical properties of the MKPCs.

3. Results and Discussion

3.1. Properties of the Magnesium Potassium Phosphate Hydrate Grown with Different Magnesia/KH₂PO₄ Molar Ratios

Magnesium oxide and KH₂PO₄ underwent an exothermic hydration reaction, and the chemical reaction schemes are shown below. The formation of MgKPO₄·6H₂O (struvite-K) has a great influence on the solidification time, yield and mechanical strength of the resulting materials.

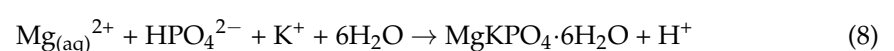
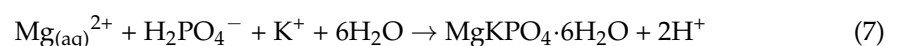
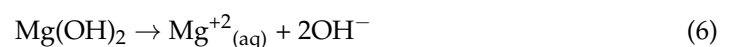
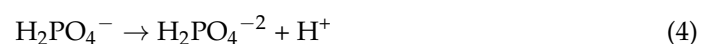


Figure 1 shows the morphology of the hydrates formed in the hydration reaction with different MgO/KH₂PO₄ ratios. By mixing magnesium oxide and KH₂PO₄ with water,

the acid-base reaction forms columnar $\text{Mg KH}_2\text{PO}_4 \cdot 6\text{H}_2\text{O}$. Figure 1a shows that at the $\text{MgO}/\text{KH}_2\text{PO}_4$ molar ratio of two, the resulting hydrate has a sheet-like morphology with loose structure. When the ratio of $\text{MgO}/\text{KH}_2\text{PO}_4$ increases and reaches four, it leads to the formation of more $\text{MgKPO}_4 \cdot 6\text{H}_2\text{O}$ (Figure 1b,c). When it exceeds four (Figure 1d), it can limit the hydration reaction with KH_2PO_4 , resulting in spherical agglomeration.

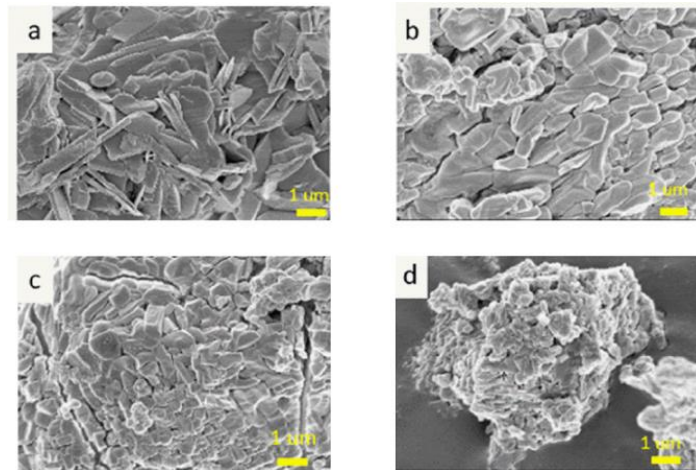


Figure 1. SEM images of $\text{MgKPO}_4 \cdot 6\text{H}_2\text{O}$ prepared with different magnesia/ KH_2PO_4 molar ratios = (a) 2, (b) 3, (c) 4, and (d) 5.

The mechanical strength of the prepared hydrate is also related to the molar ratio of $\text{MgO}/\text{KH}_2\text{PO}_4$. Figure 2a shows that the compressive strength of the obtained $\text{MgKPO}_4 \cdot 6\text{H}_2\text{O}$ increases with the molar ratio, ranging from 2–4. At a molar ratio of four, the obtained maximum value of 10.5 MPa may be due to the additional hydration products produced during the hydration reaction. It indicates that the percentage of magnesium oxide interacting with KH_2PO_4 determines the final compressive strength. The release of water during the hydration process leads to the shrinkage of the surface and the generation of cracks inside the $\text{MgKPO}_4 \cdot 6\text{H}_2\text{O}$. Figure 2b,c shows the effects of shrinkage and water absorption. Obviously, increasing the molar ratio can still cause shrinkage, even at a molar ratio of four. Likewise, as the molar ratio increases, the water absorption also increases. The adhesion between $\text{MgKPO}_4 \cdot 6\text{H}_2\text{O}$ and the steel matrix plays a crucial role in the tensile strength, as shown in Figure 2d. The most significant bond strength results from a better bonding strength of $6.62 \text{ kgf}/\text{cm}^2$ achieved at a molar ratio of four.

The potentiodynamic polarization curves and various corrosion properties (i.e., corrosion potential, corrosion current density, b_a , b_c , polarization resistance and corrosion rate) of samples with different $\text{MgO}/\text{KH}_2\text{PO}_4$ molar ratios are shown in Figure 3 and Table 3, respectively. The results show that all samples have a negative value of the corrosion potential, which are relatively small changes, with values between -0.39 and -0.58 V. The corrosion current density, the polarization resistance and the corrosion rate present a large variation in values, between 2.79 and $28 \mu\text{A cm}^{-2}$, 0.82 and $19.1 (\Omega \text{ cm}^2)$, and 0.033 and 0.34 (mm/year), respectively, which significantly reveals the corrosion behavior of the MKPCs varies with the $\text{MgO}/\text{KH}_2\text{PO}_4$ molar ratio. When the M/P molar ratio is three, the absolute value of corrosion potential, the corrosion current density and the corrosion rate obviously shifts to the lowest value, whereas the polarization resistance shifts towards the highest value, which demonstrates anti-corrosion tendency and the best corrosion resistance performance, due to the formation of a denser protective layer on the surface of steel substrate, contributed by phosphate and Fe^{2+} ions. It makes the surface of the substrate more resistant to corrosion. Various results including corrosion rate, corrosion potential, and corrosion current density, obtained at different $\text{MgO}/\text{KH}_2\text{PO}_4$ molar ratios, are listed in Table 3. Compared with the molar ratio four, molar ratio three is supposed to possess superior bonding strength. However, molar ratio four exhibited the best bond

strength, as was seen in Figure 2d. Therefore, we speculate that the packaging condition within $\text{MgKPO}_4 \cdot 6\text{H}_2\text{O}$ is influenced by the packaging density, which can create additional voids in the bulk specimen.

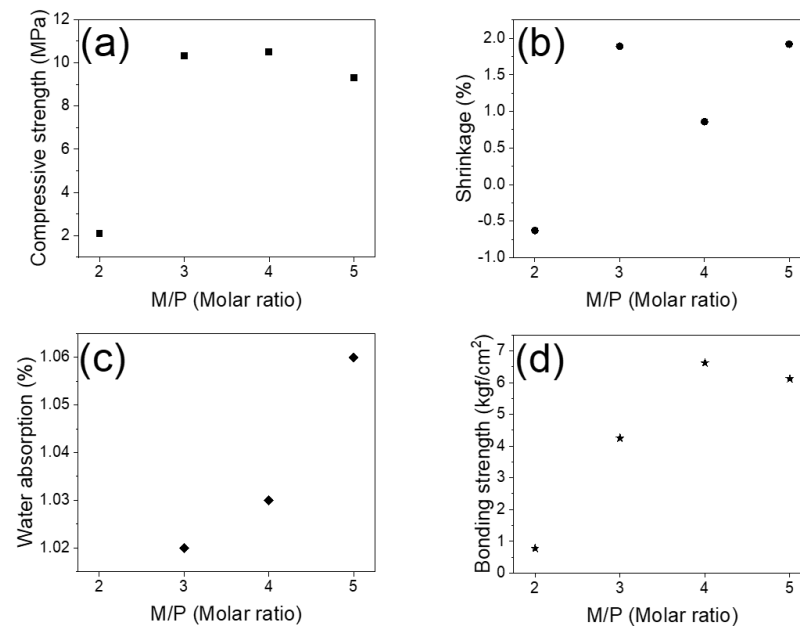


Figure 2. The properties of (a) compressive strength, (b) volume shrinkage, (c) water absorption, and (d) bonding strength of $\text{MgKPO}_4 \cdot 6\text{H}_2\text{O}$ at different magnesia/ KH_2PO_4 molar ratios after a three-hour hydration reaction in the atmosphere.

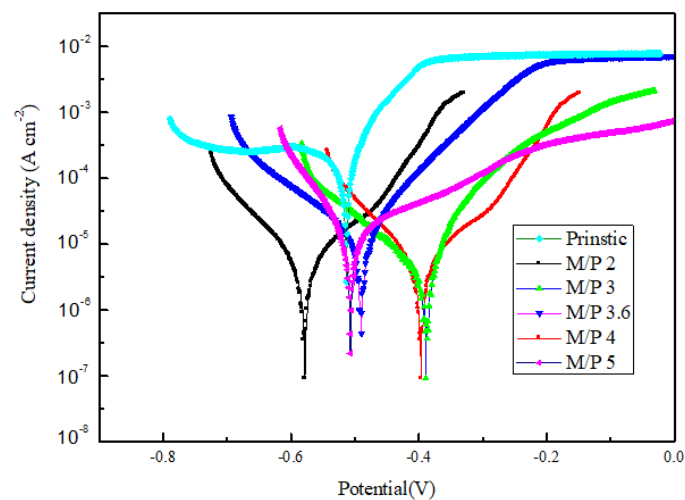


Figure 3. Potentiodynamic polarization for corrosion testing of $\text{MgKPO}_4 \cdot 6\text{H}_2\text{O}$ at different magnesia/ KH_2PO_4 molar ratios.

Table 3. Calculated parameters of $\text{MgKPO}_4 \cdot 6\text{H}_2\text{O}$ at different magnesia/ KH_2PO_4 molar ratios.

Sample	E_{corr} (V vs. SCE)	J_{corr} ($\mu\text{A cm}^{-2}$)	b_a	b_c	R_p^a ($\Omega \text{ cm}^2$)	v_p^b (mm/year)
Pristine	−0.52	28	20.2	−32.8	0.82	0.340
MP = 2	−0.58	6	9.0	−22.6	1.08	0.073
M/P = 3	−0.39	2.79	18.0	−21.1	19.1	0.033
M/P = 3.6	−0.49	4.9	12.4	−20.5	2.7	0.059
M/P = 4	−0.39	3.29	13.1	−17.7	6.7	0.040
M/P = 5	−0.50	4.9	13.2	−22.8	2.8	0.059

^a: data obtained from Equation (1). ^b: data obtained from Equation (2).

3.2. Influence of Thermal-Insulating Additives on the Flame Resistance of MKPCs

As is well known, magnesium potassium phosphate hydrate has moderate thermal-insulating properties. At high temperatures, the free water in the MKPC and the chemically-bonded water in the $\text{MgKPO}_4 \cdot 6\text{H}_2\text{O}$ dissipated a large amount of heat, which effectively retarded the spread of the fire and reduced the heat conduction of the coating. At $M/P = 4$ and $W/C = 0.8$, adding the additives, e.g., wollastonite, vermiculite, or aerogel with different contents, as in samples A1–A3, significantly enhanced the hydrate's flame resistance. Figure 4a shows that, at a weight ratio of wollastonite to vermiculite of 20:10 (named sample A1), MKPC could reduce thermal propagation across the coating by a significant amount as it was under the invasion of flame. The lowered thermal conductivity of the MKPC is significantly attributed to the introduction of thermal-insulating additives in the coating. The results in Figure 4b also show that the flame-resistance rating of MKPCs can reach 250 °C within an hour after exposure to an alcohol blast burner flame. Using the optimum composition of wollastonite and vermiculite for the formulations, MKPCs reduce their thermal conductivity, and simultaneously enhance long-term flame-resistance.

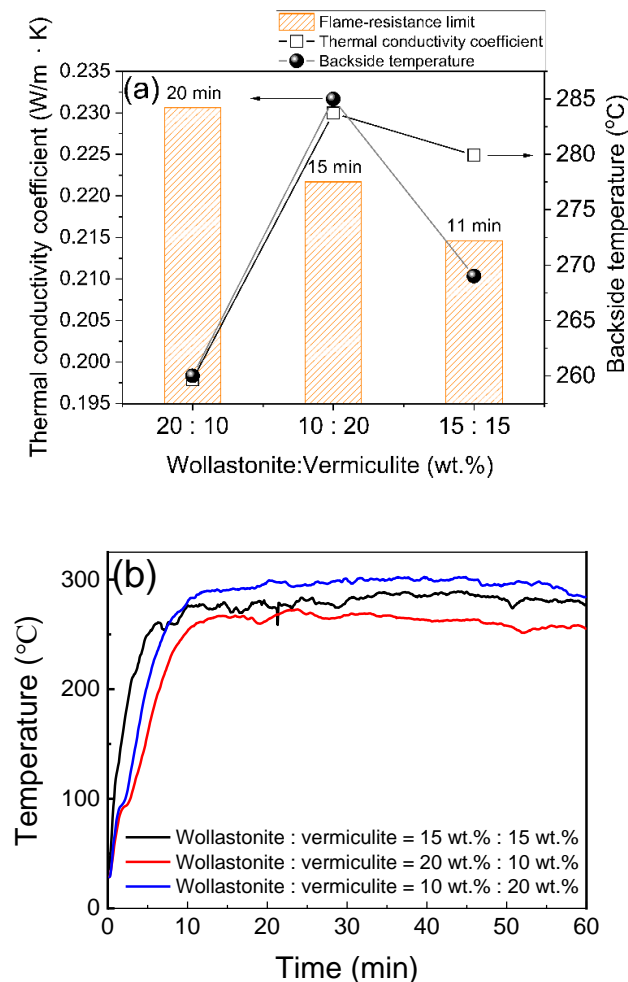


Figure 4. (a) Thermal conductivity, backside temperature for steel substrate, and flame-resistance limit; and (b) flame-resistance rating of the MKPCs with different weight ratios of wollastonite to vermiculite. (magnesia/ KH_2PO_4 molar ratio = 4).

Considering the high porosity, large surface area, and low thermal conductivity of aerogel, it could be used as a heat-capturing additive inside the MKPCs, as in samples B1–B3. As shown in Figure 5a, increasing the aerogel content leads to a gradual loss of the thermal conductivity of the MKPCs and an associated extension of the flame-resistance limit. The flame-retardancy shows that the backside temperature does not decrease linearly with

decreasing thermal conductivity and increasing aerogel content. As shown in Figure 5b, the poor mechanical properties of MKPC samples A1 and B2, such as smaller adhesive strength and compressive strength, indicate that it lacks structural integrity to withstand suitable high-temperature combustion. As a result, aerogels are not considered ideal additives in MKPC formulations.

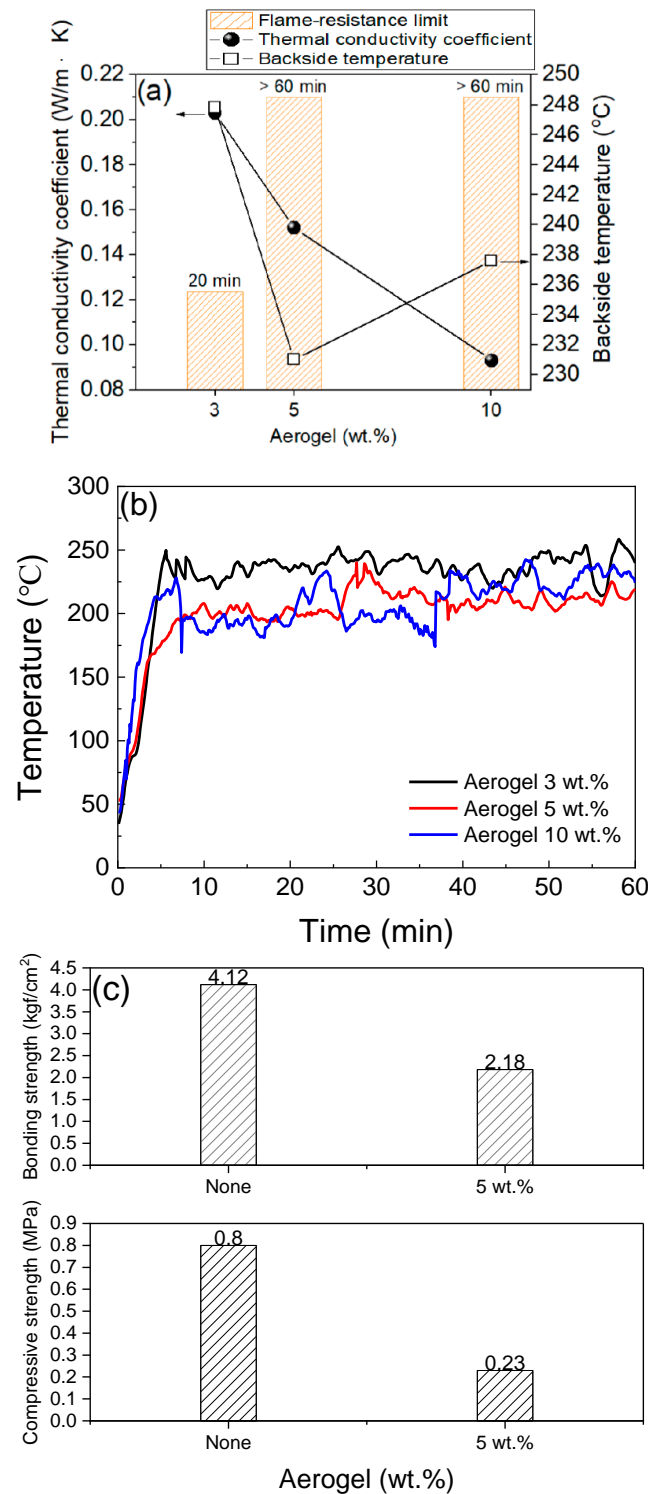


Figure 5. (a) Thermal conductivity, backside temperature for steel substrate, flame-resistance limit to different contents of aerogel and, (b) mechanical strength (c) bonding and compressive strength with 0 and 5 wt.% aerogel of the MKPCs. (magnesia/ KH_2PO_4 molar ratio = 4; wollastonite:vermiculite = 20:10 wt.%).

3.3. Mullite Whisker on the Flame Resistance and Microstructure of the MKPCs

Although the above-mentioned thermal insulation additives can enhance flame-retardancy, they still appear to affect the mechanical strength of MKPC. The carbon properties of mullite whiskers can act as heat shielding materials when exposed to flame, due to their high thermal stability, hardness and adhesive strength. The in situ growth of mullite whiskers requires active aluminum and silicon sources. Mullite whiskers are formed by combining wollastonite, aluminum hydroxide and aluminum fluoride at high temperatures. Figure 6a illustrates how MKPC samples C1–C4 extend their flame-retardancy limit by increasing the content of aluminum hydroxide. A backside temperature of 230 °C was obtained by adding aluminum hydroxide (10 wt.%) to the MKPC. In addition, the flame-retardancy ratings of different aluminum hydroxide contents of MKPC samples C1–C4 in Figure 6b are all below 275 °C, and it is considered that 10 wt.% aluminum hydroxide is the optimal level in the formulation. The thermal decomposition reaction of aluminum hydroxide is shown in Equation (7).

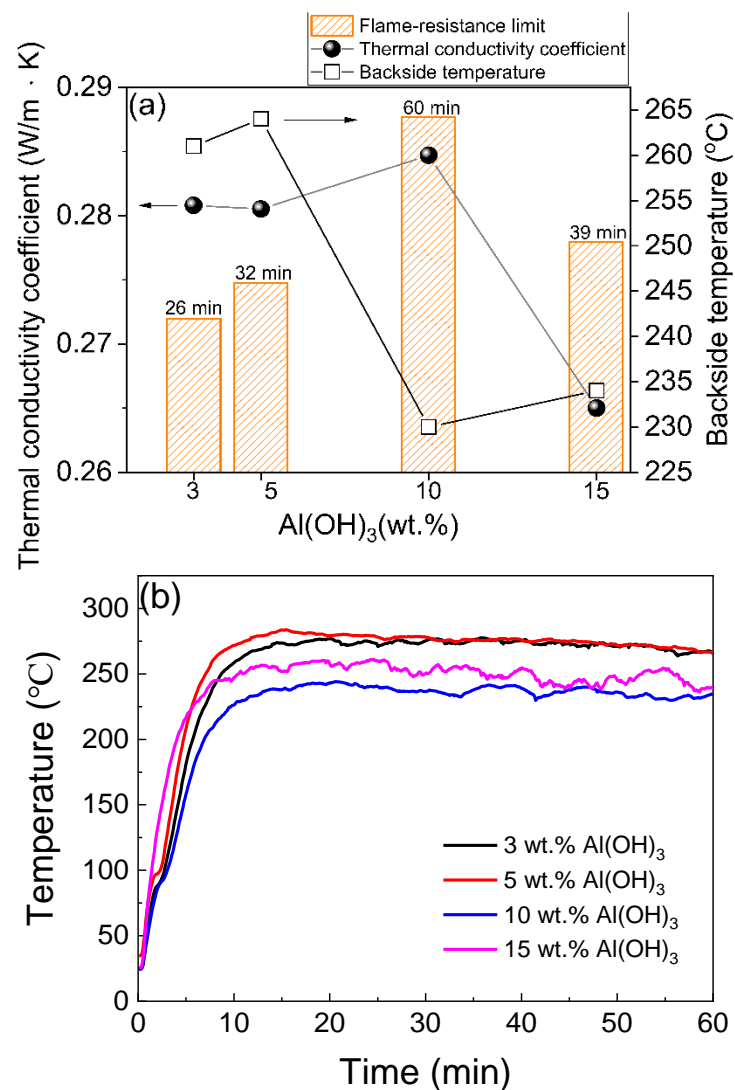
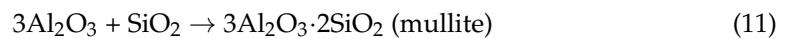
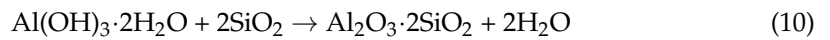


Figure 6. (a) Thermal conductivity, backside temperature for steel substrate, flame-resistance limit relating to different contents of aluminum trihydroxide, and (b) flame-resistance rating of the MKPCs. (magnesia/KH₂PO₄ molar ratio = 4; wollastonite:vermiculite = 20:10 wt.%).

The XRD patterns in Figure 7, sample C3, demonstrate the formation of mullite whiskers after 1000 °C calcination for one and three hours, respectively, and indicate that mullite whiskers can generate at high temperatures. As shown in the figure, the diffraction

peaks of magnesium oxide and $\text{MgKPO}_4 \cdot 6\text{H}_2\text{O}$ are located at 43°C and 22.5°C , respectively, and the characteristic peak of mullite appears at 28°C after calcination [19,22]. It means that aluminum hydroxide decomposes to alumina, which reacts with wollastonite to form mullite whiskers. Chemical reaction Equations (9)–(11) show how mullite is formed at $\sim 900^\circ\text{C}$.



Compared with samples not exposed to an alcohol blast burner flame, Figure 8b exhibits more compact surface morphology than that illustrated in Figure 8a, sample C3, providing an indirect explanation for the formation of mullite whiskers at high temperatures.

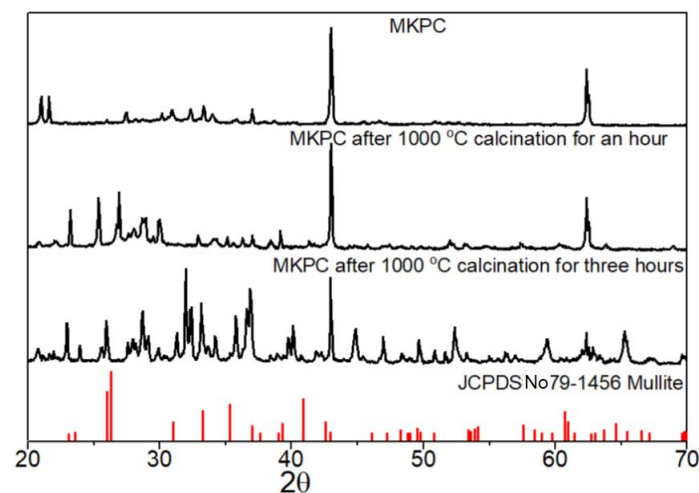


Figure 7. XRD diffractions of the MKPCs before and after the calcination at 1000°C for one and three hours, respectively.

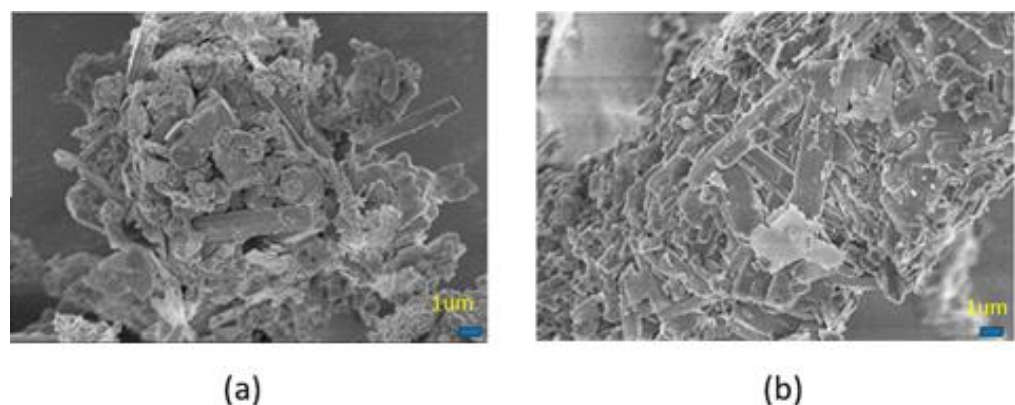


Figure 8. SEM images of the MKPCs (a) before, and (b) after calcination at 1000°C for an hour. (magnesia/ KH_2PO_4 molar ratio = 4; wollastonite:vermiculite = 20:10 wt.%; aluminum trihydroxide = 10 wt.%).

3.4. Influence of Flame-Retardant Minerals of the MKPCs

Certain minerals can effectively improve the fire resistance and mechanical properties of MKPC during flame exposure. The mineral metakaolin is used as a flame-retardant additive in MKPC formulations, considering its high flame-retardancy, flexibility and adhesion. Figure 9a shows that the thermal conductivity of MKPC samples D1–D3 decreases with the content of metakaolin. Theoretically, the thermal conductivity of MKPC is inversely proportional to the backside temperature. The corresponding fire-resistance limit first in-

creases and then decreases. With the addition of 5% metakaolin, the backside temperature of MKPC reached around 240 °C, and its flame-retardancy limit and thermal conductivity were 44 min and 0.2522 w/m·K, respectively. However, the flame-retardancy ratings in Figure 9b show that the increase in flame-retardancy of MKPC samples D1–D3 is not linear with the amount of metakaolin. From the morphology observed after heating at 1000 °C for one hour, Figure 10 shows that as MKPC samples D1–D3 had more metakaolin added, the denser their surface became. These results suggest that metakaolin is not suitable in formulating MKPCs as flame-retardants.

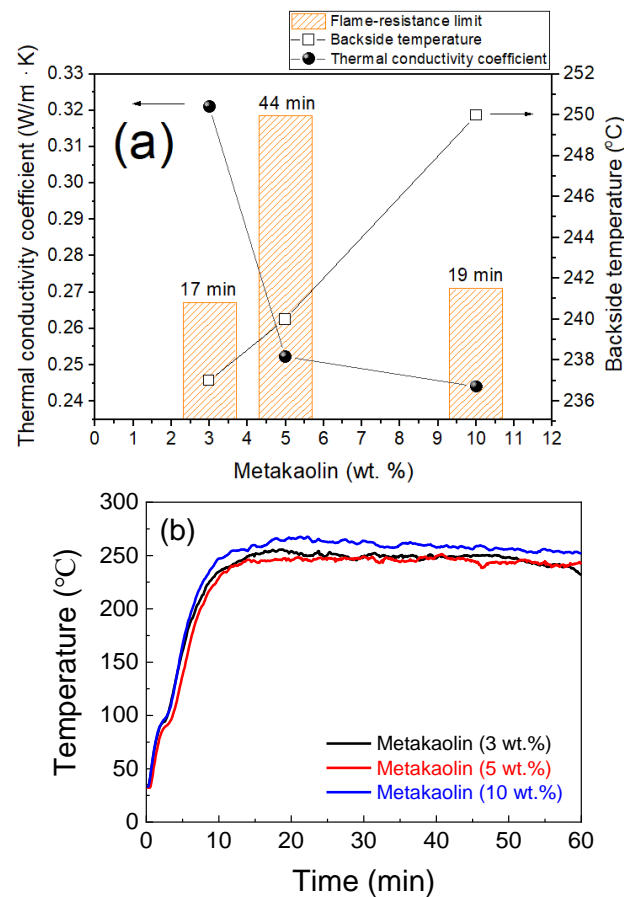


Figure 9. (a) Thermal conductivity, backside temperature for steel substrate, flame-resistance limit with respect to different contents of metakaolin, and (b) flame-resistance rating of the MKPCs. (magnesia/ KH_2PO_4 molar ratio equals to 4; wollastonite:vermiculite = 20:10 wt.%; aluminum trihydroxide = 10 wt.%).

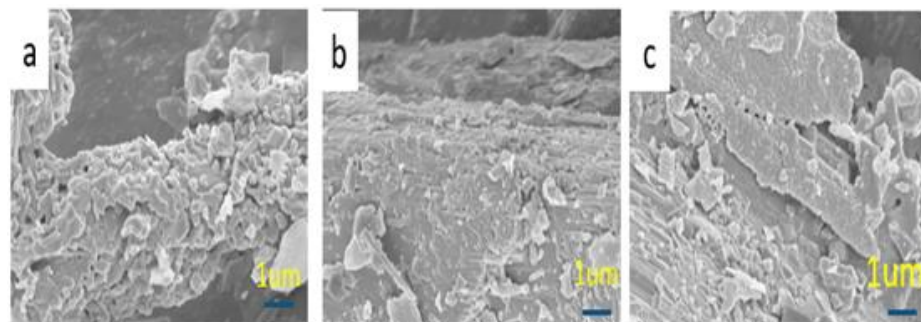
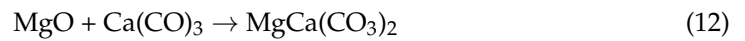


Figure 10. SEM surface images of the MKPCs with different contents of metakaolin: (a) 3, (b) 5, and (c) 10 wt.% after calcination at 1000 °C for an hour.

Alternatively, calcium carbonate can react with magnesium oxide to generate calcium magnesium carbonate, and its chemical reaction equation is as follows:



Calcium magnesium carbonate is relatively thermally stable and can decompose to carbon dioxide at high temperatures, thereby significantly reducing heat transfer from the flame to the substrate. Figure 11a shows that when the calcium carbonate content exceeds 5 wt.%, as in samples E1–E3, the flame-retardancy limit exceeds one hour. This is especially seen in the case of 5 wt.% calcium carbonate, where the thermal conductivity of MKPC is the lowest, at 0.2200 w/m·K, and the backside temperature is approximately 200 °C. Figure 12 shows that MKPC samples E1–E3, containing calcium carbonate, became denser than neat one hour after heating at 1000 °C. However, excess calcium carbonate will form excess calcium oxide, which will further react with phosphoric acid to form tricalcium phosphate, thereby inhibiting the formation of $\text{MgKPO}_4 \cdot 6\text{H}_2\text{O}$.

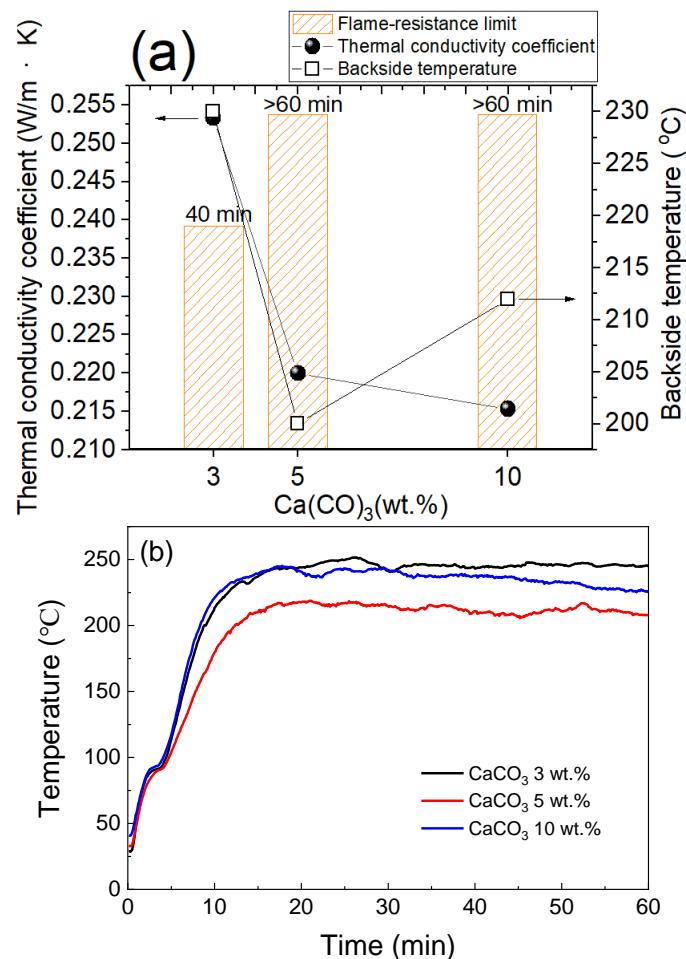


Figure 11. (a) Thermal conductivity, backside temperature, flame-resistance limit with respect to different contents of calcium carbonate, and (b) flame-resistance rating of the MKPCs (magnesia/ KH_2PO_4 molar ratio = 4; wollastonite:vermiculite = 20:10 wt.%; aluminum trihydroxide = 10 wt.%).

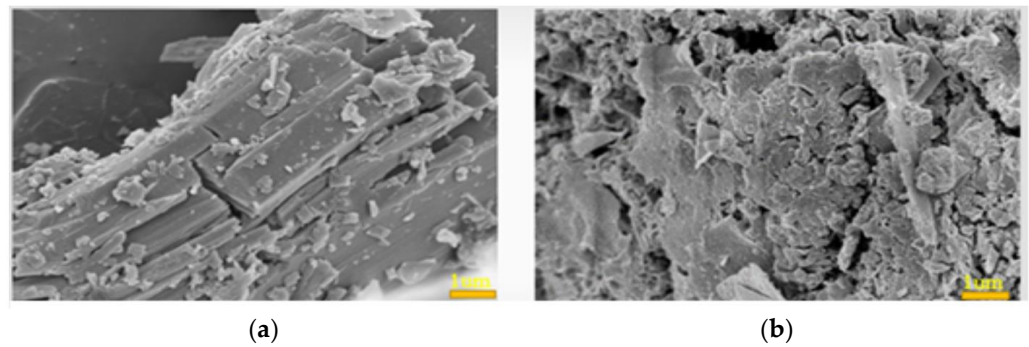


Figure 12. SEM images of flame-retardant coatings (a) before, and (b) after heating to 1000 °C for an hour. (magnesia/ KH_2PO_4 molar ratios = 4; wollastonite:vermiculite = 20:10 wt.%; aluminum trihydroxide = 10 wt.%; calcium carbonate = 5 wt.%).

3.5. Physical Properties of the MKPCs with the Optimum Additives

When developing MKPC, some basic properties such as mechanical properties, weather-resistance and flame-resistance need to be taken into consideration. The MKPC exhibited better mechanical properties when calcium carbonate was added (as per sample E2), as shown in Figure 13. Figure 14 shows visual images of MKPC sample E2 after different freeze-thaw cycles to investigate the degree of degradation under extreme conditions. None of the samples showed severe changes or deterioration such as visible cracks, peeling or blistering. The optimal composition of MKPC reduced deterioration, and sample E2 even remained intact when performing a water absorption test (Figure 15). The compact configuration of bulk samples allows minimal water vapor penetration into small voids, accumulating within the MKPC.

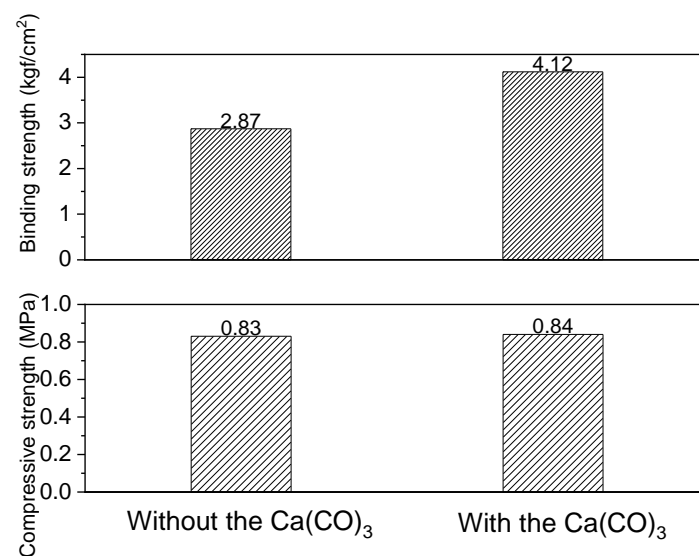


Figure 13. Mechanical properties of bonding and compressive strength of the optimum compositions of the MKPCs.

In Figure 16a, the thermal stability of MKPC sample E2 at elevated temperatures was studied by thermogravimetric analysis, which revealed several stages of weight loss during heating. Three corresponding weight losses occurred at temperatures below 200 °C, 200–300 °C and 600–700 °C, respectively, with the loss of ions/water and crystallization of the main hydration products, the endothermic decomposition of aluminum trihydroxide, and CO_2 release from calcium carbonate at high temperatures, respectively. The total residual weight loss of the MKPC after heating at 1000 °C was only 1.2 wt.%, while untreated MKPC was as high as 15 wt.%. This can be attributed to the formation of

mullite whiskers in the MKPC, improving thermal stability, mechanical strength and flame-retardancy. As shown in Figure 16b, the three-hour FR rating of the best MKPC could maintain at 420 °C throughout. Therefore, the developed MKPCs can have remarkable flame-retardant properties.

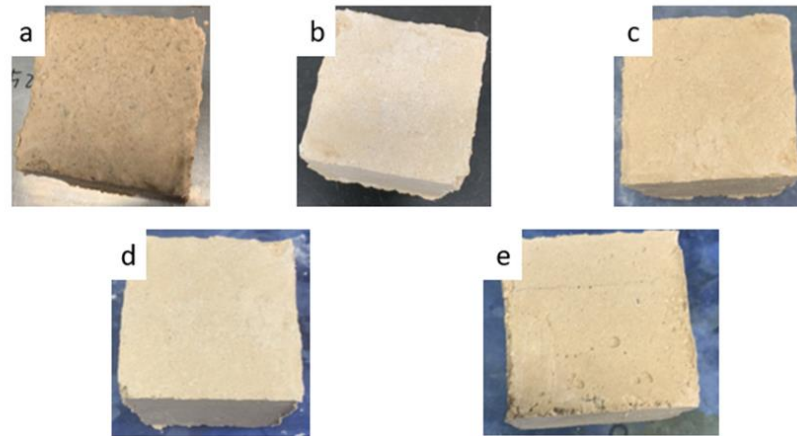


Figure 14. MKPCs with the optimum compositions (a) before and after (b) 1, (c) 5, (d) 10, and (e) 15 times freeze-thaw cycles.

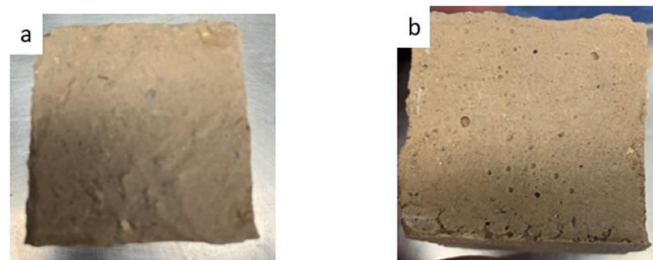


Figure 15. MKPCs with the optimum compositions (a) before, and (b) after water resistance testing for one day.

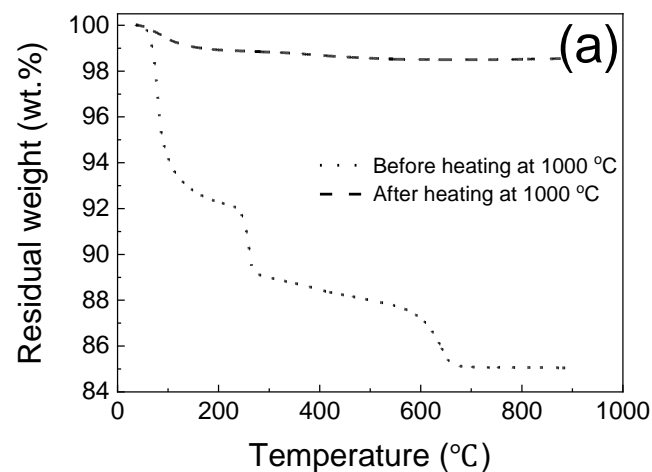


Figure 16. Cont.

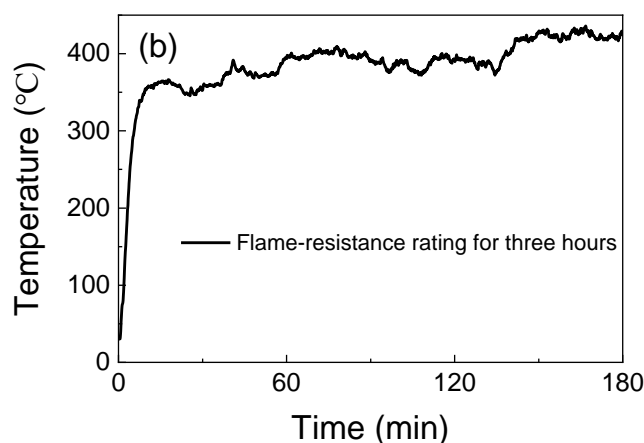


Figure 16. (a) Thermal analysis of the MKPCs before and after heating at 1000 °C, and (b) three hours of flame-resistance rating of the MKPC with the optimum compositions.

4. Conclusions

The MKPC matrix is based on $\text{MgKPO}_4 \cdot 6\text{H}_2\text{O}$. The composite material contains thermal insulation additives (wollastonite and vermiculite) and functional additives (aluminum hydroxide, aluminum fluoride and calcium carbonate). When the $\text{MgO}/\text{KH}_2\text{PO}_4$ molar ratio is four, the original compressive strength is 10.5 MPa and the bond strength is 6.62 kgf/cm², respectively. Furthermore, adding the proper amount of wollastonite, vermiculite, aluminum trihydroxide and calcium carbonate to the formulation could enhance its flame-retardancy and increase mechanical strength as well. When exposed to flame, mullite whiskers enhance shielding strength and flame-retardancy by interacting with wollastonite, aluminum trihydroxide, and aluminum fluoride at 900 °C. At the optimum composition of MKPC ($\text{MgO}/\text{KH}_2\text{PO}_4$ molar ratio = 4; wollastonite:vermiculite = 20:10 wt.%; aluminum trihydroxide = 10 wt.%; and calcium carbonate = 5 wt.%), coated on a steel substrate, the flame-resistance limit is as low as ~200 °C and the three hours flame-retardant rating reaches approximately 420 °C. In the present study, the optimum MKPC coated steel substrate provided lower thermal conductivity, better corrosion resistance, stronger compressive strength, higher bonding strength, better resistance to freezing/thawing and water, as well as excellent flame-retardancy. Despite this, the application of actual steel structure fire protection, the steel type and composition, coating characteristics and thickness, the adhesion between the coating with primer and topcoat, as well as mechanical properties and weather resistance etc., must be considered precisely, and further research is required.

Author Contributions: Conceptualization, K.-S.H. and T.-H.H.; methodology, H.-L.H. and X.-H.C.; software, Y.-J.L. and C.L.; writing—original draft preparation, S.-N.C.; writing—review and editing, K.-S.H. and S.-N.C.; visualization, C.L. and Y.-C.H.; supervision, Y.-C.H. and X.-H.C.; funding acquisition, T.-H.H. and H.-L.H. All authors have read and agreed to the published version of the manuscript.

Funding: This research received funding from MOST 111-2221-E-992-030 and MOST 109-2622-E-014-CC3 through the Minister of Science and Technology, Taiwan, ROC.

Institutional Review Board Statement: Not applicable.

Informed Consent Statement: Not applicable.

Data Availability Statement: Not applicable.

Acknowledgments: Appreciation is expressed for the use of soft-matter TEM equipment belonging to the Core Facility Center, Micro/Nano Technology Division of National Cheng Kung University (NCKU), Ministry of Science and Technology, Taiwan, ROC.

Conflicts of Interest: The authors declare no conflict of interest.

References

1. Abd El-Fattah, M.; El Saeed, A.M.; Dardir, M.; El-Sockary, M.A. Studying the effect of organo-modified nanoclay loading on the thermal stability, flame retardant, anti-corrosive and mechanical properties of polyurethane nanocomposite for surface coating. *Prog. Org. Coat.* **2015**, *89*, 212–219. [[CrossRef](#)]
2. Gobakis, K.; Kolokotsa, D.; Maravelaki-Kalaitzaki, N.; Perdikatsis, V.; Santamouris, M. Development and analysis of advanced inorganic coatings for buildings and urban structures. *Energy Build.* **2015**, *89*, 196–205. [[CrossRef](#)]
3. Puri, R.G.; Khanna, A. Influence of heat-stable filler on the thermal shielding performance of water-based intumescent fire-resistive coating for structural steel applications. *J. Coat. Technol. Res.* **2017**, *14*, 323–331. [[CrossRef](#)]
4. Chen, S.-N.; Li, P.-K.; Hsieh, T.-H.; Ho, K.-S.; Hong, Y.-M. Enhancements on Flame Resistance by Inorganic Silicate-Based Intumescent Coating Materials. *Materials* **2021**, *14*, 6628. [[CrossRef](#)] [[PubMed](#)]
5. Fang, Y.; Cui, P.; Ding, Z.; Zhu, J.-X. Properties of a magnesium phosphate cement-based fire-retardant coating containing glass fiber or glass fiber powder. *Constr. Build. Mater.* **2018**, *162*, 553–560. [[CrossRef](#)]
6. Xu, W.; Dai, J.-G.; Ding, Z.; Wang, Y. Polyphosphate-modified calcium aluminate cement under normal and elevated temperatures: Phase evolution, microstructure, and mechanical properties. *Ceram. Int.* **2017**, *43*, 15525–15536. [[CrossRef](#)]
7. Beddoe, R.E.; Dorner, H.W. Modelling acid attack on concrete: Part I. The essential mechanisms. *Cem. Concr. Res.* **2005**, *35*, 2333–2339. [[CrossRef](#)]
8. Ding, Z.; Xu, M.-R.; Dai, J.-G.; Dong, B.-Q.; Zhang, M.-J.; Hong, S.-X.; Xing, F. Strengthening concrete using phosphate cement-based fiber-reinforced inorganic composites for improved fire resistance. *Constr. Build. Mater.* **2019**, *212*, 755–764. [[CrossRef](#)]
9. Hall, D.A.; Stevens, R.; Jazairi, B.E. Effect of water content on the structure and mechanical properties of magnesia-phosphate cement mortar. *J. Am. Ceram. Soc.* **1998**, *81*, 1550–1556. [[CrossRef](#)]
10. Li, Y.; Sun, J.; Chen, B. Experimental study of magnesia and M/P ratio influencing properties of magnesium phosphate cement. *Constr. Build. Mater.* **2014**, *65*, 177–183. [[CrossRef](#)]
11. Xu, B.; Ma, H.; Li, Z. Influence of magnesia-to-phosphate molar ratio on microstructures, mechanical properties and thermal conductivity of magnesium potassium phosphate cement paste with large water-to-solid ratio. *Cem. Concr. Res.* **2015**, *68*, 1–9. [[CrossRef](#)]
12. Wang, X.; Hu, X.; Yang, J.; Chong, L.; Shi, C. Research progress on interfacial bonding between magnesium phosphate cement and steel: A review. *Constr. Build. Mater.* **2022**, *342*, 127925. [[CrossRef](#)]
13. Yang, Q.; Zhu, B.; Zhang, S.; Wu, X. Properties and applications of magnesia-phosphate cement mortar for rapid repair of concrete. *Cem. Concr. Res.* **2000**, *30*, 1807–1813. [[CrossRef](#)]
14. Ma, H.; Xu, B.; Liu, J.; Pei, H.; Li, Z. Effects of water content, magnesia-to-phosphate molar ratio and age on pore structure, strength and permeability of magnesium potassium phosphate cement paste. *Mater. Des.* **2014**, *64*, 497–502. [[CrossRef](#)]
15. Ji, T.; Lin, X.J.; Qiu, J.H. A Kind of Potassium Magnesium Phosphate Cement Fire-Proof Coating for Tunnels and Using Method Thereof. CN Patent 104230305B, 30 June 2016.
16. Yang, J.M.; Mei, X.X.; Sun, H.C.; Zhao, Y.D. Potassium Magnesium Phosphate Cement Base Fire-Resistant Coating for Steel Structure and Preparation Method Thereof, Application Method. CN Patent 106497157B, 18 December 2018.
17. Rashad, A.M. Vermiculite as a construction material-A short guide for Civil Engineer. *Constr. Build. Mater.* **2016**, *125*, 53–62. [[CrossRef](#)]
18. Khan, R.I.; Ashraf, W. Effects of ground wollastonite on cement hydration kinetics and strength development. *Constr. Build. Mater.* **2019**, *218*, 150–161. [[CrossRef](#)]
19. Wang, M.; Dong, X.; Zhou, Q.; Feng, Z.; Liao, Y.; Zhou, X.; Du, M.; Gu, Y. An engineering ceramic-used high-temperature-resistant inorganic phosphate-based adhesive self-reinforced by in-situ growth of mullite whiskers. *J. Eur. Ceram. Soc.* **2019**, *39*, 1703–1706. [[CrossRef](#)]
20. Zoltowski, P. On the electrical capacitance of interfaces exhibiting constant phase element behaviour. *J. Electroanal. Chem.* **1998**, *443*, 149–154. [[CrossRef](#)]
21. Lins, V.d.F.C.; de Andrade Reis, G.F.; de Araujo, C.R.; Matencio, T. Electrochemical impedance spectroscopy and linear polarization applied to evaluation of porosity of phosphate conversion coatings on electrogalvanized steels. *Appl. Surf. Sci.* **2006**, *253*, 2875–2884. [[CrossRef](#)]
22. Chong, L.; Yang, J.; Shi, C. Effect of curing regime on water resistance of magnesium-potassium phosphate cement. *Constr. Build. Mater.* **2017**, *151*, 43–51. [[CrossRef](#)]